Protoplasma (1998) 201: 158–171

PROTOPLASMA

Calmodulin is uniformly distributed during cell division in living stamen hair cells of *Tradescantia virginiana*

J. W. Vos* and **P. K. Hepler**

Plant Biology Graduate Program, Biology Department, University of Massachusetts, Amherst, Massachusetts

Received September 11, 1997
Accepted December 1, 1997

Summary. Because the activity of calmodulin (CaM) may be dependent upon its structural distribution, we have examined its spatial localization in living cells. We have focused on cell division and cell plate formation, where conventional immunofluorescence studies report that CaM is specifically associated with microtubules (MTs) of the spindle and the phragmoplast. In dividing stamen hair cells of *Tradescantia virginiana* that were injected with fluorescently labeled CaM and examined by confocal laser scanning microscopy (CLSM), we found that the labeled protein is uniformly distributed throughout the cell and is not localized with the phragmoplast MTs or any other obvious structure. To explore why these images from live cells differ from those prepared by immunolabeling, we investigated the fate of CaM during fixation and compared it with the localization of fixable dextran and tubulin. The results show that fixation causes severe changes in cell morphology and in the distribution of CaM and dextran in three quarters of the cells. Conversely, injected rhodamine-tubulin did not show redistribution after fixation. We conclude that in the live cell, CaM is largely uniformly distributed throughout the cytoplasm, and secondly that conventional chemical fixation does not preserve CaM, and probably many other soluble proteins, in its in vivo distribution. The role postulated for CaM in mitosis, solely based on indirect immunofluorescence microscopy, has to be re-evaluated.

Keywords: Accessible volume; Calmodulin; Cell division; Fixation; Fluorescent-analog cytochemistry; *Tradescantia*.

Abbreviations: BSA bovine serum albumin; CaM calmodulin; CLSM confocal laser scanning microscopy; Cy3 indocarbocyanine; EDTA ethylenediamine-tetraacetic acid; EGTA ethylene glycol bis (β-aminoethyl ether)-N,N,N′N′-tetraacetic acid; FITC fluorescein-isothiocyanate; IAF 5-iodoacetamido-fluorescein; MT microtubule; PBS phosphate-buffered saline; TBS Tris-buffered saline.

*Correspondence and reprints: Biology Department, Morrill Science Center, University of Massachusetts, Amherst, MA 01003, U.S.A.
E-mail: jwvos@bio.umass.edu

Introduction

CaM is a highly conserved calcium-binding protein that functions in many eukaryotic signaling pathways to shape and pass on signals encoded in temporally and spatially defined calcium concentrations (for reviews, see Rhoads and Friedberg 1997, James et al. 1995, Means 1994, Török and Whitaker 1994, Cohen and Klee 1988a). In plants many functions for calmodulin have been found that are similar to those in animal cells, however, some special binding targets and activities have been described as well (Poovaiah and Reddy 1993, Roberts and Harmon 1992, Braam 1992, Allen and Hepler 1989), including a CaM-binding form of the microtubule motor protein kinesin (KCBP) (Reddy et al. 1996). Following the discovery of CaM, considerable attention has been focused on its binding targets and how a ubiquitous, conserved protein like CaM with multiple interactions can be a regulatory key component. Its localization in cells and tissues has been investigated, with the view that its differential spatial distribution could contribute to specific functions. From immunofluorescent labeling studies it has been reported that CaM is localized to the mitotic apparatus in various vertebrate cell lines (Mitsuyama and Kanno 1993, Welsh and Sweet 1989, Dedman et al. 1982, Welsh et al. 1978). In some studies CaM localization to the cytoplasmic microtubules was found only after extracting mammalian cells with detergents (Deery et al. 1984).

In pea and onion root tip cells, CaM has been localized to the interzone of the spindle during anaphase

and to the phragmoplast, but not to the preprophase band (Wick 1990, Wick et al. 1985). Therefore CaM may be involved in regulation of these two dynamic microtubule (MT) arrays, but not in regulation or the formation of the preprophase band. Vantard et al. (1985), on the other hand, found CaM in *Haemanthus* endosperm within the polar MT converging centers, but not within the phragmoplast, in patterns distinct from those of MTs. They suggested a role for CaM in the regulation of kinetochore MT dynamics, i.e., spindle formation, MT disassembly, and chromosome movement.

Unfortunately, all the above studies were carried out on fixed and permeabilized cells, and as a consequence, a protein like CaM, which is largely soluble, may have suffered extensive redistribution (Melan and Sluder 1992). Although association of fluorescein-CaM with the mitotic apparatus has been reported in live animal cells (Welsh and Sweet 1989, Stemple et al. 1988, Zavortink et al. 1983, Hamaguchi and Iwasa 1980), the influence of the light path length and the accessible volume has not been addressed adequately in these studies. The spindle and the phragmoplast are devoid of larger organelles, such as mitochondria and dictyosomes, and thus contain relatively more cytosol. Every cytoplasmic molecule will therefore display a "higher concentration" in these regions. Moreover these earlier studies have not benefitted from confocal laser scanning microscopy (CLSM) (Hepler and Gunning 1998).

Here we report on the localization of CaM in living stamen hair cells of *Tradescantia virginiana* during mitosis, cytokinesis and interphase and compare it with the data on the distribution of dextran as a volume marker. Our results show that CaM is not localized with any MT array but is merely distributed according to the accessible cytoplasmic volume in the cell. Cells that were injected with labeled CaM or dextran and then chemically fixed, generally showed severe and artifactual redistribution of these soluble fluorescent probes. The distribution of labeled tubulin on the other hand did not show any redistribution after fixation. When chemical and cryofixation where compared with the live cell distribution it was clear that chemical fixation did not conserve the live cell distribution of CaM.

Material and methods

Plant material

Tradescantia virginiana plants were grown at 22 °C/18 °C during an 18 h light cycle in a growth chamber. For injection experiments young stamen hairs were prepared from immature flower buds as described in Vos et al. (1998), Valster and Hepler (1997) and Hepler and Callaham (1987). For quantitative Western blot analysis, young buds of inflorescences were used.

Pressure micro-injection

Stamen hairs were injected as described by Vos et al. (1998). In brief, stamen hairs were dissected and immobilized in 1% low gelling temperature agarose VII (Sigma, St. Louis, MO) in *Tradescantia* stamen hair culture medium (5 mM Hepes, pH 7.0, 1 mM KCl, 1 mM $MgCl_2$, 0.1 mM $CaCl_2$) and 0.025% Triton X-100 on HF treated or poly-L-lysine (1 mg/ml) coated coverslips mounted on slides. Cells were pressure injected with precision micromanipulators (Narishige, Greenvale, NY and Newport, Irvine, CA) and capillary glass needles (World Precision Instruments, Sarasota, FL) mounted in a pressure syringe system (Eppendorf, Brinkmann, Westbury, NY and Gilmont Instruments, Barrington, IL). Needles were filled with indocarbocyanine(Cy3)-labeled bovine CaM (D. L. Taylor and A. H. Gough), 5-iodoacetamido-fluorescein (IAF) (Molecular Probes, Eugene, OR) labeled spinach CaM (Sigma), fluorescein-labeled 10 kDa neutral dextran (Molecular Probes) or lysine fixable Texas-red-labeled 10 kDa dextran (Molecular Probes) in concentrations ranging from 0.3 to 1.0 mg/ml in 0.5 mM Tris or PIPES with 0.75 mM NaCl, pH 7.0–7.5. Rhodamine-labeled tubulin (Cytoskeleton, Denver, CO) was injected at 0.2–0.25 mg/ml in 20 mM glutamate, 0.5 mM $MgSO_4$, 1.0 mM EGTA, pH 7.0. Images were taken with an argon or krypton/argon CLSM (MRC600; Bio-Rad, Hercules, CA) mounted on an upright or inverted Zeiss microscope (Zeiss, Thornwood, NY) or an inverted Nikon microscope (Nikon, Melville, NY) equipped with a ×40 wide angle, noncorrected Nikon Fluor 1.3 NA oil immersion lens. Small corrections for bleed-through between the two photomultipliers were only used with images captured with the argon laser. Images were processed by Adobe Photoshop 3.0 (Adobe, San Jose, CA).

Quantitative Western blot analysis

Total protein extraction

Endogenous CaM concentrations were determined from total protein extracts from *Tradescantia* inflorescences based on plant CaM purification protocols (Anderson 1983). Young flower buds were ground in liquid nitrogen and the powder was added to hot (85–90 °C) extraction buffer (50 mM Tris, 150 mM NaCl, 5 mM $MgSO_4$, 5 mM EGTA, 2% SDS, 10 mM DTT). After boiling for 5 min and quickly cooling, the mixture was centrifuged at 16,000 **g** for 30 min at 4 °C. Protein in the supernatant was precipitated with 4 volumes of cold (–20 °C) acetone for 1 h, and centrifuged at 16,000 **g** for 30 min. After rinsing with cold acetone, pellets were dried under vacuum for 40 min and resuspended in 50 mM Tris, 150 mM NaCl, 0.02% NaN_3.

SDS-PAGE and Western blotting

Total *Tradescantia* protein extracts and standards of doubling dilutions (0.625 to 20 μg/ml) of purified spinach CaM (Sigma) were run on 17.5% SDS-PAGE (sodium dodecyl sulfate-polyacrylamide gel electrophoresis) gels. Protein was transferred to polyvinylidene difluoride membranes (Hulen et al. 1991) in potassium phosphate buffer (25 mM KH_2PO_4/K_2HPO_4, pH 7.0) at 10–20 V for 16 to 20 h. Membranes were fixed for 45 min at room temperature with 0.2% glutaraldehyde in above buffer, followed by a blocking step in 5%

BSA in TBS for 3 h at room temperature or overnight at 4 °C. Primary antibody (IgG monoclonal anti-carrot CaM from mouse, clone 1D10; R. Cyr) (Fisher and Cyr 1993) was applied 1 : 500 in TBS with 1% BSA for 2 h at room temperature. Secondary antibody (alkaline phosphatase-conjugated goat anti-mouse; Boehringer Mannheim Biochemicals, Indianapolis, IN) was applied 1 : 2000 in above buffer with 0.05% Tween-20 (w/v) for 2 h at room temperature. Enzyme substrates, nitro blue tetrazolium chloride (NBT) and 5-bromo-4-chloro 3′ indolylphosphate *p*-toluidine (BCIP) in Tris buffer (Pierce, Rockford, IL), were applied according to manufacturer's instructions.

Quantification

Computer images of membranes were analyzed with PipScan (J. G. Kunkel) and Origin (Microcal, Northampton, MA). In brief, pixel values (0–255) of protein bands were converted to 8 averaged columns (band width): 2 bands of unknown concentrations of *Tradescantia* CaM and 6 spinach CaM standards. The final total-band pixel intensities were determined by plotting the intensities of the band lengths, subtracting the background and summing the pixel values under the curve.

Total protein assay

Total protein concentrations were determined by a Lowry (1951) assay as modified by Schacterle and Pollack (1973).

Statistical analysis of mitotic transition times

Medians of minimal metaphase transition times, as determined from the first observation after nuclear-envelope breakdown to the start of anaphase, and anaphase transition times, from the separation of chromatids to the start of the phragmoplast formation, of bovine CaM- and dextran-injected cells were compared by the Mann–Whitney U-test for small samples sizes (Campbell 1974).

Labeling of spinach CaM with IAF and Ca^{2+} shift assay

Purified spinach CaM (Sigma) was labeled at the only cysteine at position 27 (Friedberg 1990) with IAF (Zot et al. 1990). 10 mg of IAF per ml dimethylformamide was added at 10× molar excess to 1 mg of CaM per ml 50 mM Tris, 75 mM NaCl, pH 7.5, 1 mM EDTA, 1–2 mM DTT, and 0.01% NaN_3, and incubated at 4 °C overnight. A Microcon-30 microconcentrator (Amicon, Beverly, MA) was blocked with 1% BSA, 0.1% NaN_3, and 0.05% Tween 20 in PBS for 2 h at room temperature, and than carefully rinsed with 50 mM Tris and 75 mM NaCl, pH 7.5. The IAF-CaM mixture was loaded on the filter, centrifuged at 16,800 **g** for 20 min at 4 °C, and washed twice while centrifuging with Tris-buffer to remove free dye. The retentate was retrieved by inverting the filter and centrifuging it for 10 min at 67,200 **g**. The supernatant, ca. 0.7 mg of CaM-IAF per ml in Tris-buffer, was stored at 4 °C. To test Ca^{2+} binding, IAF- and unlabeled spinach CaM was incubated with 5 mM $CaCl_2$ or 5 mM EGTA for 5 min before adding SDS-sample buffer. Samples were run on standard SDS-PAGE gels and transferred to polyvinylidene difluoride membranes for Western blotting (see above).

Fluorescent analog cytochemistry followed by chemical fixation

After injection of Cy3-CaM, IAF-CaM, lysine-fixable Texas red-dextran (10 kDa) or rhodamine-tubulin as described above, stamen hairs were chemically fixed and processed as for whole-cell indirect immunofluorescent labeling (Larsen and Wolniak 1993). CLSM imaging of the distribution of fluorescent analogs was continued during these steps. In brief, stamen hairs were fixed for 30 min to 1 h with 3.7% formaldehyde (from stock), 4% paraformaldehyde (made fresh from powder), or 4% paraformaldehyde and 0.1% glutaraldehyde in PIPES, magnesium, EGTA buffer (8 mM PIPES, 1 mM $MgSO_4$, 1 mM EGTA, pH 7.0), or *Tradescantia* culture medium. In some instances the cuticle and cell wall were digested with a mixture of 0.1% cutinase (InterSpex Products, Foster City, CA), 0.5% pectolyase, 1% Onozuka cellulase, 1% macerase, 1% cellulysin, 0.4 M D-mannitol and 0.05% Nonidet P-40 in PIPES, magnesium, EGTA buffer for 1 h. All stamen hairs were continued to be bathed in above buffer or culture medium with 1% Nonidet P-40 for up to 20 h.

Indirect immunofluorescent labeling of sectioned material

Tradescantia stamen hairs were cryofixed on agar or formvar coated loops in liquid propane (Lancelle et al. 1986) or fixed chemically with 4% paraformaldehyde or 4% paraformaldehyde and 0.1% glutaraldehyde in *Tradescantia* culture medium, embedded in butylmethylmethacrylate mix and prepared for immunofluorescent labeling (Baskin et al. 1992, 1996). Cryofixed material was substituted in acetone at –80 °C, with or without postfixation with 4% paraformaldehyde, 0.1% glutaraldehyde, or both. Chemically fixed material was substituted at room temperature. 2 μm thick sections were cut with glass knives and immunofluorescently labeled for CaM or tubulin. In brief, the embedment was dissolved with acetone for 30 min, free aldehyde residues were neutralized with 1% $NaBH_4$ for 30 min, and nonspecific binding sites were blocked with 1% BSA, 0.1% NaN_3, 0.05% Tween 20 in PBS for 1 h at 37 °C. Primary antibodies were applied as follows: monoclonal mouse anti-carrot CaM IgG, clone 1D10 (R. Cyr) undiluted, and monoclonal mouse anti-chicken α-tubulin IgG1, clone DM1A (Sigma) 1 : 100 in blocking solution, both for 2 h at 37 °C or overnight at 4 °C. Secondary antibody, Cy3-conjugated goat anti-mouse IgG (Boehringer Mannheim), was applied 1 : 200 in blocking solution, for 2 h at 37 °C or overnight at 4 °C. Sections were embedded in VectaShield (Vector Laboratories, Burlingame, CA) and imaged with CLSM.

Results

Localization of labeled calmodulin and dextran in living cells

To ascertain the localization of CaM in the living cell, stamen hair cells of *Tradescantia virginiana* were injected with low concentrations of bovine Cy3-CaM at various phases of cell division. The incorporation of exogenous CaM into the cell was fast, within 30 s, did not depend on the phase of the cell cycle, and did not visibly affect or halt cytoplasmic streaming in interphase cells. In total, 27 successful injections with bovine Cy3-CaM were performed of which 2 were into interphase cells, 6 into prophase, 16 into metaphase, and 3 into anaphase. All cells stayed alive and all but 4 cells injected during metaphase or anaphase went on to the next mitotic phase. A typical example is shown in Fig. 1, in which a cell was injected during prometaphase with Cy3-CaM at a needle concentration of 0.3 mg/ml and followed by CLSM as it contin-

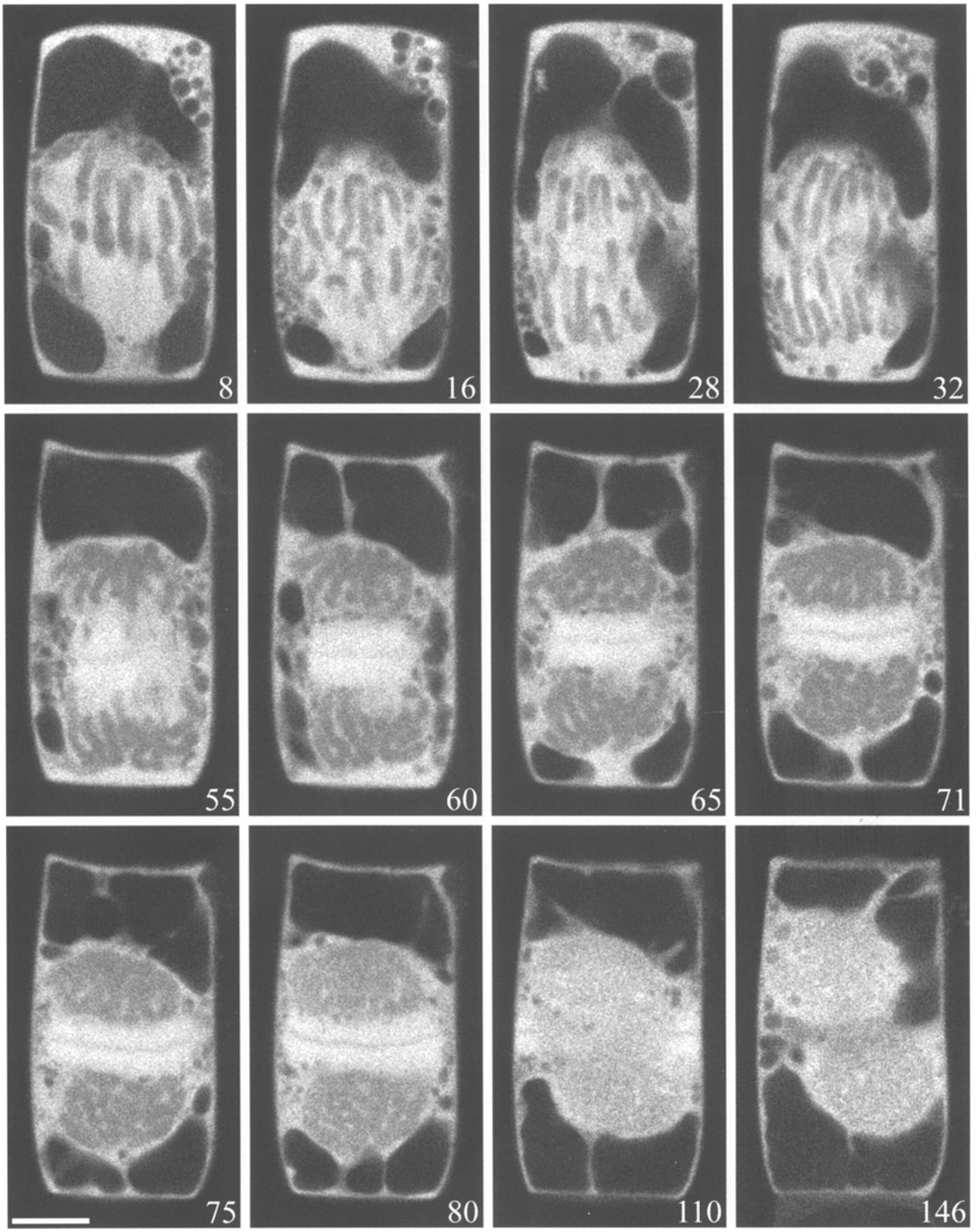

Fig. 1. Cy3-calmodulin localization during cell division. A stamen hair cell in prometaphase was injected with a needle concentration of 0.3 mg of Cy3-CaM per ml and followed by CLSM. Numbers on the panels are minutes after injection. Metaphase: 8 min after injection, anaphase: 16 to 32 min, telophase: 55 to 110 min, interphase: 146 min. The distribution of CaM is uniform in the cytoplasm, but appears nonspecifically excluded from the chromosomes, and concentrated in the phragmoplast. This is due to variations in the accessible volume (see Fig. 2). Bar: 10 μm

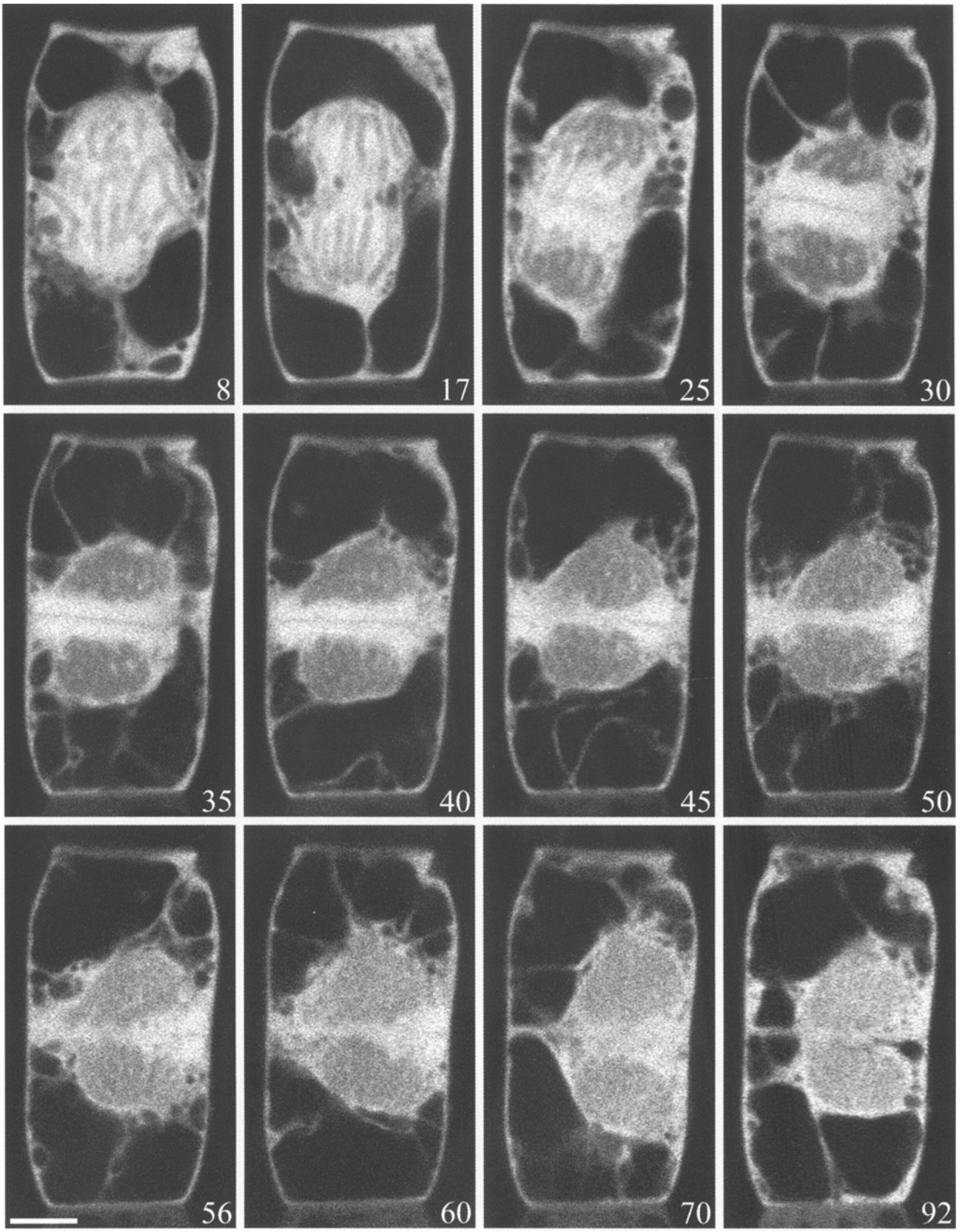

Fig. 2. Fluorescein-dextran localization during cell division. A prometaphase cell was injected with 0.2 mg of fluorescein-dextran (10 kDa) per ml and followed by CLSM. Numbers on the panels are minutes after injection. Anaphase: 8 to 17 min after injection, telophase: 25 to 70 min, interphase: 92 min. The localization of dextran corresponds to the accessible volume that varies between regions of the cytoplasm. Note the similarity in fluorescence distribution with the cell injected with CaM (Fig. 1). Bar: 10 μm

ued mitosis (from 8 to 32 min after injection) and completed cytokinesis (from 55 to 110 min) within 2 h. The Cy3-CaM permeated through the cytosol and was only excluded from vacuoles and regions in the cytoplasm occupied by chromosomes and large organelles. During late telophase (110 min after injection), as the phragmoplast widened and a torus of MTs is formed, the CaM also seemed to be relocated to this area. After cytokinesis, the two newly formed nuclei appeared more fluorescent than the chromosomes did during telophase but slightly less than the surrounding cytoplasm due to the decondensing of the chromatin (146 min after injection). In this regard CaM, while it is not concentrated in the nuclei, neither is it excluded.

Because CaM appeared to concentrate in the phragmoplast region (Fig. 1, from 60 to 80 min) it became important to determine the underlying cause. In previous work with BSA (Zhang et al. 1990) and $p13^{suc1}$ (Hepler et al. 1993), similar phragmoplast accumulations were observed that could be attributed to the increased accessible volume created by the palisade of MTs, which excludes large organelles. To correct for variations in accessible volume, stamen hair cells were injected with 10 kDa fluorescein-dextran, an inert volume marker. In total, 14 cells were successfully injected and followed through cell division. All showed the same distributions for dextran as were found for CaM. Figure 2 shows a cell injected with 0.2 mg of fluorescein-dextran per ml during prometaphase that was followed through cell division (from 8 to 70 min after injection). The 10 kDa fluorescein-dextran was not taken up by the vacuoles, nor did it leak out of the protoplast or spread to neighboring cells. The dextran concentration within the chromosomes was lower than in the surrounding cytoplasm due to the reduced accessible volume of condensed chromatin. During telophase, dextran was concentrated in the phragmoplast, possibly caused by the exclusion of larger organelles by the dense array of MTs. However, a dark line at the cell plate indicated that, as with CaM, dextran has been excluded from the nascent cell plate.

When CaM and dextran with different fluorescent labels were injected together into dividing stamen hair cells, the two images were nearly identical (Fig. 3) and could be superimposed (not shown). Thus injection of small amounts of labeled CaM into stamen hair cells shows that the protein is uniformly spread throughout the accessible cytoplasmic volume during any phase of the cell cycle (Fig. 1) as illustrated with the injection of the volume marker fluorescein-dextran (Fig. 2). There is no specific localization of CaM with any structure in the dividing cell. Its localization thus is completely unlike that of injected labeled tubulin (compare with Fig. 6 i, k) (Zhang et al. 1990, 1992; Valster and Hepler 1997).

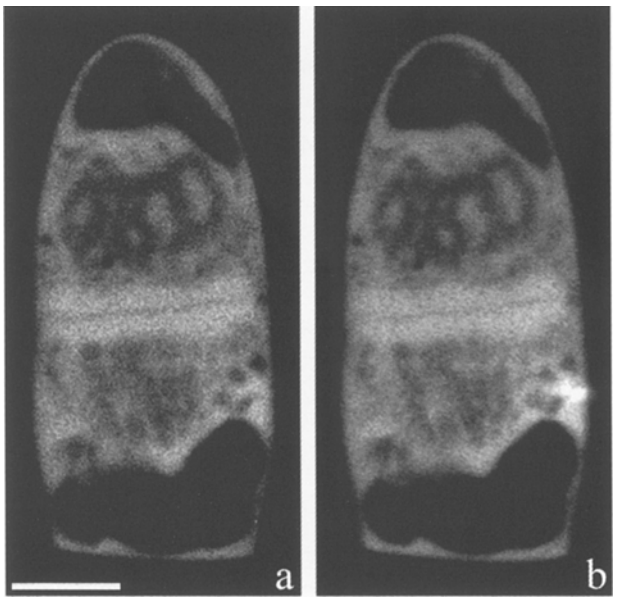

Fig. 3 a, b. Colocalization of calmodulin and dextran. A stamen hair cell was injected during telophase with 0.5 mg of Cy3-CaM per ml mixed with 0.5 mg of FITC-dextran (10 kDa) per ml. The distribution of Cy3-CaM (**b**) is similar to that of FITC-dextran (**a**) except at the site of injection where some of the CaM seems to be trapped in the wound plug. It can be reasoned from this and like images that the CaM distribution is uniform throughout the cytoplasm. Gain and black level of both photo multiplier tubes on the MRC600-CLSM were adjusted to give similarly bright images, but otherwise the images were not separately enhanced. Bar: 10 μm

Quantitative Western blot analysis of endogenous CaM concentrations

To test if the total CaM concentration was not swamped by the injected analog, the endogenous cytoplasmic concentration was determined by densitometry of Western blottings of total protein extracts of *Tradescantia* flower buds and standards of purified CaM from spinach (Fig. 4). Both *Tradescantia* CaM (Fig. 4 a, lanes 1 and 2) and doubling dilutions of spinach CaM (Fig. 4 a, lanes 3 to 7) were recognized by the carrot CaM antibody and were identical in size. The standard curve (Fig. 4 b) shows the two *Tradescantia* samples and five dilutions of spinach CaM from the above membrane. Extrapolation of the two unknown samples resulted in concentrations of ca. 3.0

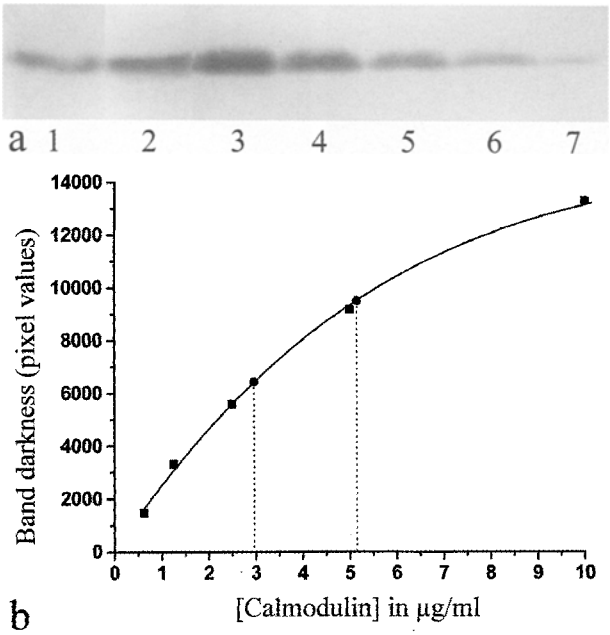

Fig. 4 a, b. Quantitative analysis of endogenous calmodulin. The endogenous *Tradescantia* CaM concentration was compared to known dilutions of spinach CaM. **a** Western blot showing single bands of two total protein samples of *Tradescantia* flower buds (*1* and *2*) and five bands of doubling dilutions (10 to 0.625 µg/ml) of purified spinach CaM (*3* to *7*) probed with carrot CaM-antibody. **b** Band darkness (pixel intensity) of the standard dilution samples (■). The CaM concentrations of the two *Tradescantia* samples (●) are extrapolated to be ca. 3.0 µg/ml and ca. 5.1 µg/ml

µg/ml and ca. 5.1 µg/ml. The average concentration of CaM, from three measurements with two protein samples, was ca. 4 µg/ml. This is equivalent to ca. 20 µg CaM per gram fresh weight, ca. 0.5 mg CaM per gram total protein as determined by a Lowry assay, or to a cytoplasmic concentration of ca. 11 µM (assuming the cytoplasm constitutes 10% of the average cell volume). These amounts agree with concentrations found in other plant tissues (Allen and Hepler 1989, Muto and Miyachi 1984, Anderson 1983). Pressure injection increased the CaM concentration by about 6%, if we assume that in dividing cells the vacuole occupies 50% of the total cell volume of 10 pl, and that injection adds about 1% to it (Zhang

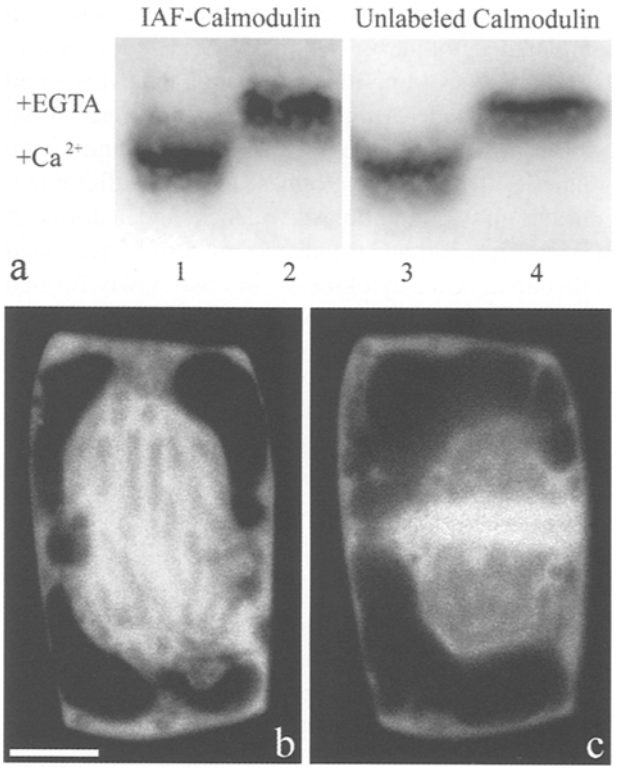

Fig. 5 a–c. Calcium shift assay and localization of spinach IAF-CaM. **a** Western blotting of CaM incubated with either 5 mM Ca^{2+} (*1* and *3*) or 5 mM EGTA (*2* and *4*) suggests that the labeled spinach CaM (*1* and *2*) is able to bind Ca^{2+} as its mobility is equal to the unlabeled spinach CaM (*3* and *4*). **b** and **c** A metaphase cell was injected with 0.5 µg of IAF-CaM per ml, and followed through anaphase, 24 min after injection (**b**), and telophase, 47 min after injection (**c**). Spinach CaM, potentially highly homologous to *Tradescantia* CaM, has a similar, uniform distribution as bovine CaM (Fig. 1) and dextran (Fig. 2). Bar: 10 µm

et al. 1990). Thus we concluded that the endogenous pool was not dominated by the injectate.

Mitosis transition times of injected cells

Because CaM activity could be involved in cell division and MT stability (Keith et al. 1983, Lee and Wolff 1982), we verified that indeed injection of small amounts did not alter mitotic transition times.

Fig. 6 a–l. Redistribution and differential extraction of CaM and dextran after chemical fixation. Cells were injected with 0.5 mg of Cy3-CaM (**a–d**), 0.5 mg of 10 kDa Texas red, lysine-fixable dextran (**e–h**), or 0.2–0.25 mg of rhodamine-tubulin (**i–l**) per ml, and imaged before (a, c, e, g, i, and k) and after fixation (b, d, f, h, j, and l). In three quarters of the injected cells, the CaM or dextran redistributes to the chromatin, nucleoli, phragmoplast, and cell plate (**b** and **f**). Only in a quarter of the cells is the distribution similar to that of the live cell (**d** and **h**), although morphological artefacts are still visible. By contrast, redistributions of this kind are not seen when tubulin-injected cells are fixed (**j** and **l**). Bar: 10 µm

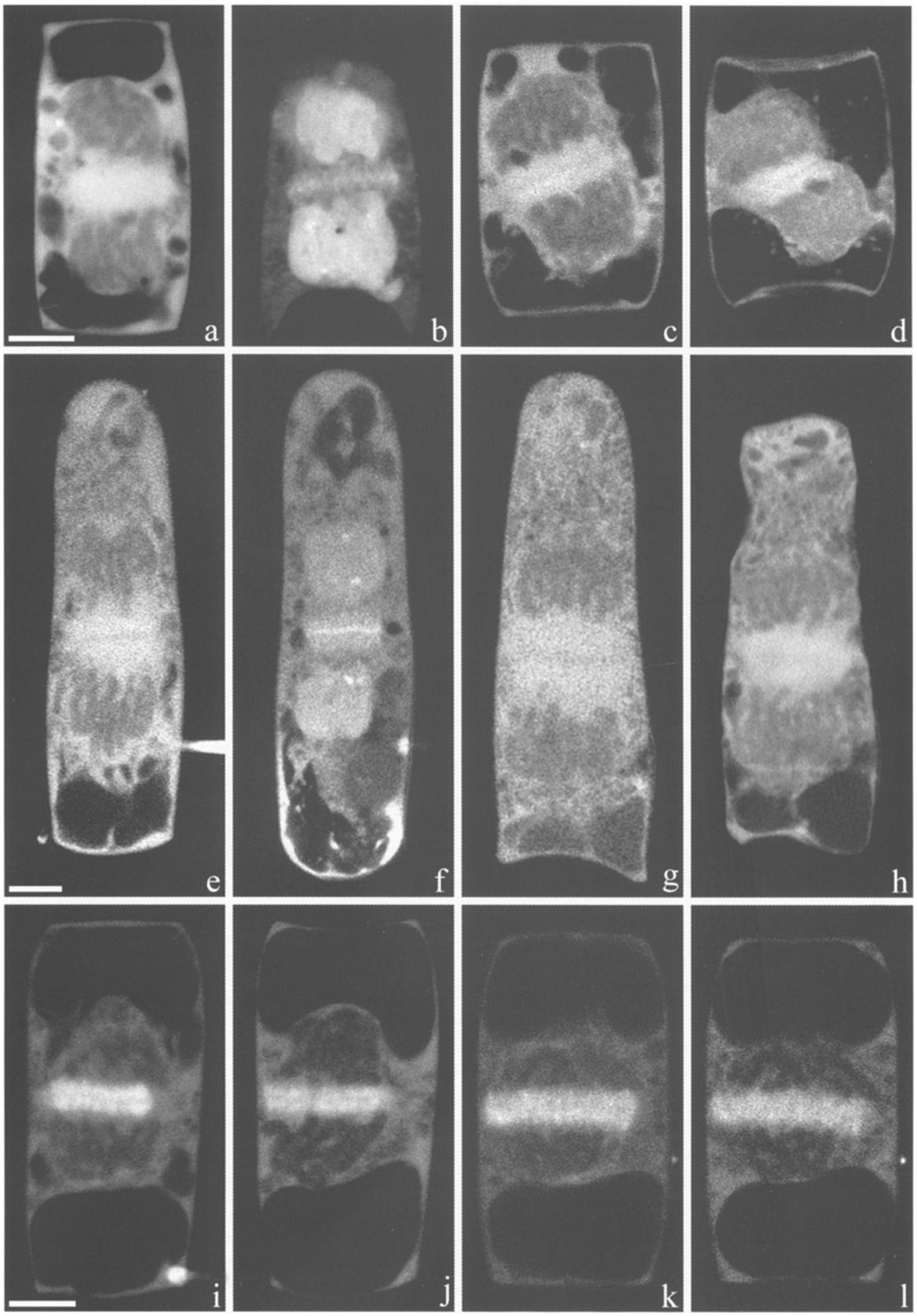
a
b
c
d
e
f
g
h
i
j
k
l

Both metaphase and anaphase transition times were found to be similar between cells injected with CaM or dextran as tested by the Mann–Whitney U-test. The median of the minimal length of metaphase in CaM-injected cells, as measured from first observation during prometaphase to the separation of the chromatids, was 26 ± 6 min, and in dextran-injected cells 29 ± 10 min. Anaphase, from the separation of the chromatids to the phragmoplast formation, in CaM-injected cells had a median length of 25 ± 7 min and in dextran-injected cells a length of 24 ± 4 min.

Localization of labeled spinach CaM

To determine if CaM from a more closely related source would behave similarly to injected bovine CaM, we labeled commercially available spinach CaM with IAF, tested its capability to bind calcium (Fig. 5 a), and injected it into stamen hair cells (Fig. 5 b, c). Both IAF-labeled and unlabeled spinach CaM showed a calcium-dependent conformational change of equal magnitude under denaturing conditions. When calcium was bound, the protein moved faster on SDS-PAGE gels (Fig. 5 a, lanes 1 and 3) due to its active, globular form. If incubated with EGTA before adding sample buffer and electrophoresis, the protein moved more slowly (Fig. 5 a, lanes 2 and 4) due to its inactive state, i.e., dumbbell shape. All 11 successful injections of this spinach CaM preparation showed the same uniform distribution as with Cy3-labeled bovine CaM or FITC-dextran. Figure 5 b and c shows a cell injected in prometaphase and followed through anaphase (Fig. 5 b), 24 min after injection, and telophase (Fig. 5 c), 47 min after injection.

Redistribution and differential extraction of CaM and dextran after chemical fixation

To determine why CaM in chemically fixed cells appears to be colocalized with the mitotic apparatus (Vantard et al. 1985), or the phragmoplast (Wick et al. 1985), we followed the fate of fluorescently labeled CaM, 10 kDa lysine-fixable dextran or tubulin in living and chemically fixed cells. Standard procedures were used as if the cells were being prepared for antibody labeling including fixation with paraformaldehyde and glutaraldehyde (Wick and Duniec 1986), and treatment with wall-digestive enzymes and/or detergents (Larsen and Wolniak 1993). The results show that the distribution of the injected CaM and dextran changed dramatically during and after fixation (Fig. 6), with three quarters of the cells showing abnormal distributions, including leakage of CaM and dextran into the vacuole or neighboring cells, and movement of CaM and dextran onto the chromosomes, nucleoli, phragmoplast, and cell plate (Fig. 6 b, f). These redistributions were independent of the method of fixation and post-treatment. Only in a quarter of the cells (4 out of 16 injections for CaM, and 2 out of 8 injections for dextran) was the distribution of either CaM or dextran the same before and after fixation (compare Fig. 6 c with d, and g with h). In contrast, rhodamine-labeled tubulin, which had incorporated into the phragmoplast array (Fig. 6 i, k), did not show redistribution after fixation (Fig. 6 j, l), although cells did show morphological artefacts (5 cells injected). It is also important to note that the process of fixation, which took 1–2 min to halt cytoplasmic streaming, causes distortions in the cell morphology including loss of the turgid appearance, disappearance of cytoplasmic strands, wrinkling of the cell wall, shrinking of the spindle halves, and loss of distinctive cytoplasmic zonation associated with the phragmoplast.

Comparison of cryofixed and chemically fixed sections, labeled with CaM and tubulin antibodies

Lastly, to compare the fluorescent-analog cytochemistry approach with previous results on fixed cells, the distribution of CaM was compared between cryofixed and chemically fixed material (Fig. 7). Stamen hairs were cryofixed in liquid propane and prepared for immunolabeling (see Material and methods). Thin sections of this material (Fig. 7 a, b, e, and f) were compared with chemically fixed material subjected to the same post-fixational procedures as the cryofixed material (Fig. 7 c, d, g, and h). In general, cells kept their live cell morphology better after cryofixation. The turgid appearance was not lost, the chromosomes kept their live cell size, cytoplasmic strands were visible in most medial sections and the cell walls and plasma membranes were not wrinkled.

The labeling of CaM in cryofixed cells during telophase (Fig. 7 a) and interphase (Fig. 7 e) was generally similar to the live cell distribution of CaM and unlike that of tubulin during telophase (Fig. 7 b) or interphase (Fig. 7 f). The cytoplasm was uniformly labeled, chromosomes and nuclei appeared darker, and the phragmoplast was more intensely labeled, similar to the live cell distribution. The only difference from the live cell distribution was an accumulation of CaM antibody at the cell plate in many sec-

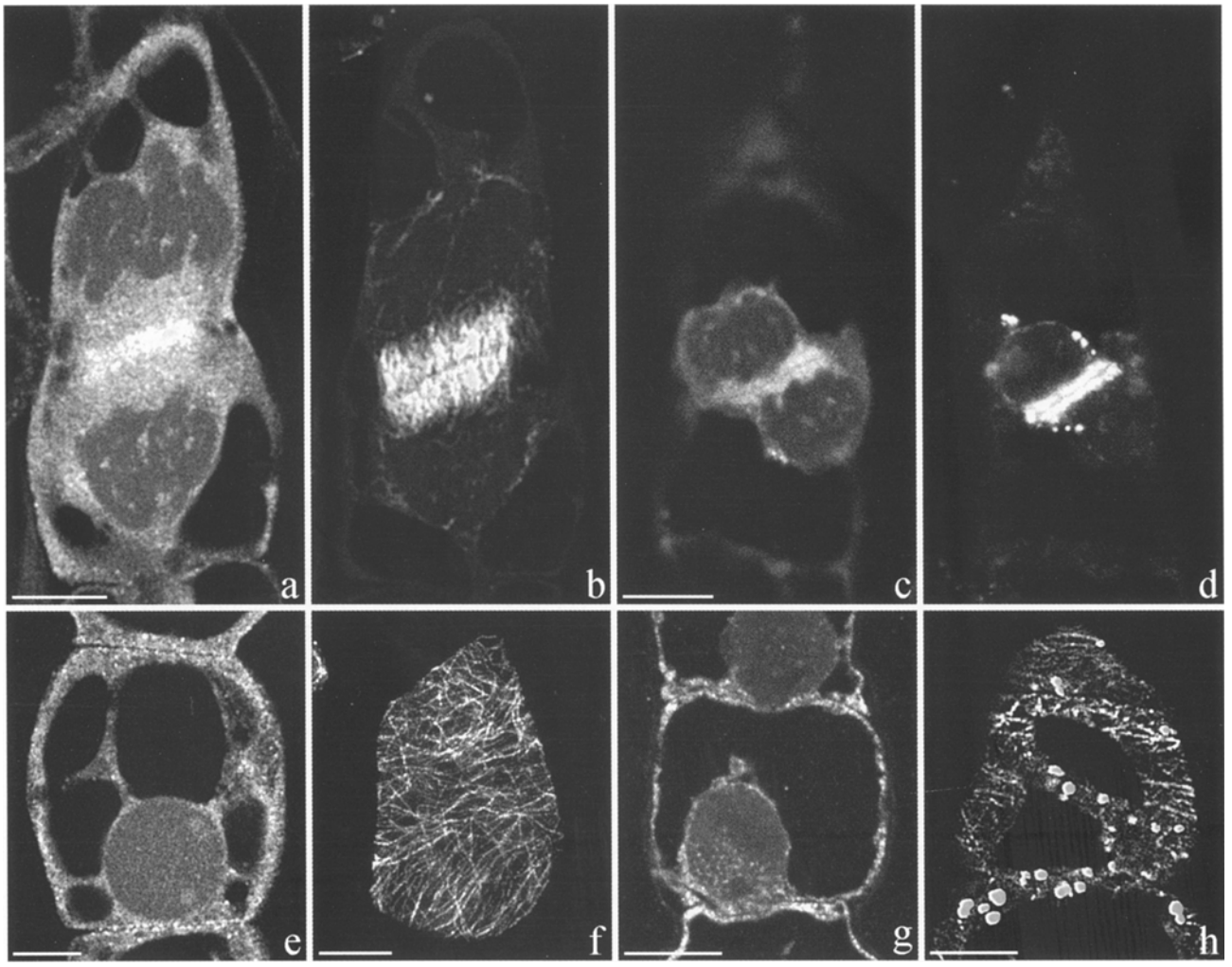

Fig. 7 a–h. Comparison of cryofixed and chemically fixed material. Cryofixed (**a, b, e,** and **f**) or chemically fixed (**c, d, g,** and **h**) sections of telophase cells (**a, b, c,** and **d**) and interphase cells (**e, f, g,** and **h**) were labeled with anti-CaM (**a, c, e,** and **g**) or anti-tubulin (**b, d, f,** and **h**). Both the CaM localization and the morphological preservation show the superiority of cryofixation over chemical fixation. The CaM distribution in cryofixed cells is largely uniform throughout the cytoplasm (**a** and **e**) and differs greatly from the tubulin localization (**b** and **f**), although the cell plate is brightly stained with the CaM antibody (**a**). In chemically fixed telophase cells CaM (**c**) and tubulin (**d**) colocalize, but not in interphase cells (**g** and **h**). **a** and **b** and **c** and **d** Sections of the same cells. Bar: 10 μm

tions. Including fixatives during substitution did not noticeably affect the overall quality of preservation or the CaM labeling.

By contrast, CaM labeling in chemically fixed cells during telophase (Fig. 7 c) was very much like the tubulin distribution (Fig. 7 d), being almost exclusively within the phragmoplast, and little or no labeling of the cortical cytoplasm. In interphase cells, CaM labeling (Fig. 7 g) was generally uniformly, along the partly collapsed cortical and perinuclear cytoplasm. Tubulin labeling in interphase cells (Fig. 7 h) was similar to the labeling in cryofixed cells although with more artefacts, such as a loss of clearly defined microtubules in medial sections. Controls in which first or both antibodies were omitted only showed weak fluorescence of agar and cells (not shown).

Discussion

Calmodulin is uniformly dispersed throughout the cytoplasm in the live cell

In contradiction to earlier work (Wick et al. 1985, Vantard et al. 1985), which reported that CaM is localized to the mitotic apparatus and the phragmoplast, our results show that CaM is uniformly distributed throughout the plant cell during all phases of

the cell cycle. Injection of small amounts of fluorescently labeled bovine or spinach CaM (Figs. 1 and 5) indicated the same distribution as injected dextran (Fig. 2), an inert polysaccharide that if injected will percolate throughout the cytosol. Injecting both probes together into one cell (Fig. 3) also revealed clearly that CaM and dextran have similar distributions. That the injectate was not merely streaming around the cytoplasm in surplus was shown by quantitative Western blot analysis of the endogenous CaM concentration (Fig. 4) together with estimates of the amounts of injectate. The results indicate that less than 10% exogenous CaM has been added, and this is unlikely to dominate the endogenous cytoplasmic pool. In addition we emphasize that the amount of CaM injected had no effect on the progression of meta- and anaphase or on cytoplasmic streaming.

The high concentration of CaM observed in the phragmoplast is due to the larger accessible volume within that region, where a dense palisade of MTs excludes large organelles like mitochondria, dictyosomes, and vacuoles (Gunning 1982), creating a zone into which small, unbound components can freely percolate. These properties of the phragmoplast can give the illusion that CaM is concentrated therein but in reality the concentration of the protein is the same throughout the entire cytosol, a conclusion strongly supported by the colocalization of fluorescent dextran. In drug experiments in which MTs were depolymerized, CaM localization was also affected (Sweet et al. 1989, Stemple et al. 1988). However, because the accessible volume is largely maintained by the cytoskeleton, the distribution of any soluble protein is likely to change if MTs (or actin microfilaments) are destabilized, especially in a structure like the phragmoplast. Likewise, preparatory processes, such as those used for *Haemanthus* endosperm cells (Vantard et al. 1985), might change the accessible volume and cause differences observed in the CaM localization between these cells and pea and onion cells (Wick et al. 1985) when fixed.

Our results do not deny a role for CaM in cell division, nor that it could be bound to certain components such as MT-binding proteins or kinesin light chains which have structural or functional associations with the cytoskeleton (Fisher et al. 1996, Matthies et al. 1993, Gratzer and Baines 1988). If (indirect) binding to the cytoskeleton occurs, these events involve a small population of the total endogenous CaM pool and are too small to be detected by the method used here.

CaM and dextran are redistributed and differentially extracted during chemical fixation

The discrepancy between the apparent uniform distribution of CaM in the cytoplasm of the live cell and the results with indirect immuno-localization studies on chemically fixed cells has been examined by fluorescent analog cytochemistry of living cells followed by fixation (Fig. 6), as used previously by Melan and Sluder (1992) to examine the distribution of selected proteins in animal cells. Their conclusion was that for proteins that form polymers like actin and tubulin most chemical fixations are sufficiently fast and stable to use, but for soluble or transiently soluble proteins like ovalbumin, BSA, and β-lactoglobulin B in vivo distribution is not conserved. Proteins were redistributed and/or differentially extracted during the preparation of cells to yield artifactual association with the nucleus, nucleoli, perinuclear region, and centrosomes. Also, after fixation the fluorescently labeled proteins displayed a fibrous, reticulate texture not observed in living cells (Melan and Sluder 1992). We similarly found erroneous, artefactual localizations of CaM and dextran to the phragmoplast, cell plate, chromatin, and nucleoli after various chemical fixations. In marked contrast, the localization of tubulin did not change during fixation. The CaM localization in live cell images was always consistent whereas the results from chemically fixed cells varied widely; cell plates in identically treated preparations could exhibit positive or negative localization of CaM.

CaM is known to be a "sticky" protein that can interact with hydrophobic regions of many proteins (Cohen and Klee 1988b). During the first minutes of conventional chemical fixation, as the regulation of Ca^{2+} and CaM interactions is being destroyed, Ca^{2+} influx could activate nonphysiological amounts of CaM that subsequently bind to fixation-stable structures, such as MTs, by means of nonspecific interactions.

Chemical versus cryofixation

The discrepancy in CaM localization between the live and fixed cell was also examined by comparing structural rearrangements in the protein distribution between conventional chemically fixed and cryofixed cells probed with antibodies (Fig. 7). In contrast to chemical fixation, cryofixation gave an excellent preservation of the cell morphology and the cytoplasmic distribution of CaM was maintained. Only in sections of telophase cells was there a redistribution of some

of the CaM to the cell plate unlike that in the live cell. This concentration might be due to antigen redistribution during substitution, although addition of fixatives during substitution did not prevent it. Alternatively the elevated concentration of CaM might represent a membrane-bound, nonexchangeable pool of CaM that is accessible to antibodies but not to fluorescent analog cytochemistry. Generally, cryofixation has been shown to be an excellent method for preserving the cellular structure and for indirect immunofluorescent labeling of MTs and actin microfilaments (Baskin et al. 1996), and even though it does not produce identical results to the live cell, still it is probably the best choice if micro-injection is not an option.

Consequences for CaM function

The implication from these observations is that it is not possible to determine the function of CaM from its overall localization. We therefore are forced to reassess models that propose a role for the protein as a regulator of mitosis (Wick et al. 1985) and kinetochore MT dynamics (Vantard et al. 1985), as both suggestions were initially and primarily based on the localization of CaM in chemical fixed material. The protein may indeed function in these events but other live-cell data are needed, such as the spatial and temporal distribution of Ca^{2+}-activated CaM (Hahn et al. 1992) and response element-bound CaM (Gough and Taylor 1993). We presume that bound CaM will represent a small, but crucial fraction of the total CaM pool, which may be governed in part, at least, by a spatially localized release of Ca^{2+}.

Conclusions

We conclude that CaM is uniformly distributed throughout the cytoplasm and that chemical fixation techniques in combination with indirect immunolocalization do not necessarily preserve and represent in vivo distribution of this protein. Studying CaM localization in chemical fixed material is not suitable for elucidating CaM functions or to base functional models upon, and in general, this approach is not preferred to demonstrate soluble-protein-dependent effects. As alternative procedures we promote fluorescent-analog cytochemistry, green-fluorescent-protein cytochemistry, or cryofixation in combination with immuno-localization at the light- or electron-microscopy level as superior methods for faithfully preserving detailed structural relationships (Hepler and Gunning 1998, Valster and Hepler 1997, Staehelin and Hepler 1996, Miller et al. 1996, Baskin et al. 1996, Hush et al. 1994), and especially the distribution of proteins that are soluble.

Acknowledgements

We thank Drs. D. L. Taylor and A. H. Gough (Carnegie Mellon University, Pittsburgh, PA) for their generous gift of Cy3-labeled bovine calmodulin, Dr. R. J. Cyr (Pennsylvania State University, University Park, PA) for his generous gift of carrot calmodulin antibodies and Dr. B. E. S. Gunning (Australian National University, Canberra, Australia) for the use of his laboratory facilities, where this project was started during the sabbatical leave of PKH. We also thank Dr. J. G. Kunkel (University of Massachusetts, Amherst, MA) and Dr. P. B. O'Hara (Amherst College, MA) for helpful discussion and G. R. Hackett for his technical assistance. This work has been supported by a grant from the USDA (agreement no. 94-37304-1180) and a senior Fulbright fellowship from the Australian-American Educational Foundation to PKH, and by a grant from the NSF (no. BBS-8714235) to the University of Massachusetts Microscopy Facility.

References

Allen E, Hepler PK (1989) Calmodulin and calcium-binding proteins. In: Marcus A (ed) The biochemistry of plants: a comprehensive treatise, vol 15. Academic Press, San Diego, pp 455–484

Anderson JM (1983) Purification of plant calmodulin. In: Means AR, O'Malley BW (eds) Methods in enzymology, vol 102, hormone action, part G, calmodulin and calcium-binding proteins. Academic Press, New York, pp 9–17

Baskin TI, Busby CH, Fowke LC, Sammut M, Gubler F (1992) Improvements in immunostaining samples embedded in methacrylate: localization of microtubules and other antigens throughout developing organs in plants of diverse taxa. Planta 187: 405–413

– Miller DD, Vos JW, Wilson JE, Hepler PK (1996) Cryofixing single cells and multicellular specimens enhances structure and immunocytochemistry for light microscopy. J Microsc 182: 149–161

Braam J (1992) Regulation of expression of calmodulin and calmodulin-related genes by environmental stimuli in plants. Cell Calcium 13: 457–463

Campbell RC (1974) Statistics for biologists, 2nd edn. Cambridge University Press, London

Cohen P, Klee CB (eds) (1988a) Calmodulin: molecular aspects of cellular regulation, vol 5. Elsevier, Amsterdam

– – (1988b) Criteria required to demonstrate calmodulin-dependent effects in vivo. In: Cohen P, Klee CB (eds) Calmodulin: molecular aspects of cellular regulation, vol 5. Elsevier, Amsterdam, pp 357–364

Deery WJ, Means AR, Brinkley BR (1984) Calmodulin-microtubule association in cultured mammalian cells. J Cell Biol 98: 904–910

Dedman JR, Welsh MJ, Kaetzel MA, Pardue RL, Brinkley BR (1982) Localization of calmodulin in tissue culture cells. In: Cheung (ed) Calcium and cell function, vol 3. Academic Press, New York, pp 455–472

Fisher DD, Cyr RJ (1993) Calcium levels affect the ability to immunolocalize calmodulin to cortical microtubules. Plant Physiol 103: 543–551

– Gilroy S, Cyr RJ (1996) Evidence for opposing effects of

calmodulin on cortical microtubules. Plant Physiol 122: 1079–1087

Friedberg F (1990) Species comparison of calmodulin sequences. Protein Seq Data Anal 3: 335–337

Gough AH, Taylor DL (1993) Fluorescence anisotropy imaging microscopy maps calmodulin binding during cellular contraction and locomotion. J Cell Biol 121: 1095–1107

Gratzer WB, Baines AJ (1988) Calmodulin and cytoskeletal function. In: Cohen P, Klee CB (eds) Calmodulin: molecular aspects of cellular regulation, vol 5. Elsevier, Amsterdam, pp 329–340

Gunning BES (1982) The cytokinetic apparatus: its development and spatial regulation. In: Lloyd CW (ed) The cytoskeleton in plant growth and development. Academic Press, London, pp 229–292

Hahn K, DeBiasio R, Taylor DL (1992) Patterns of elevated free calcium and calmodulin activation in living cells. Nature 359: 736–738

Hamaguchi Y, Iwasa F (1980) Localization of fluorescently labeled calmodulin in living sea urchin eggs during early development. Biomed Res 1: 502–509

Hepler PK, Callaham DA (1987) Free calcium increases during anaphase in stamen hair cells of *Tradescantia*. J Cell Biol 105: 2137–2143

– Gunning BES (1998) Confocal fluorescence microscopy of plant cells. Protoplasma 201: 121–157

– Sek FJ, John PCL (1993) Nuclear concentration and mitotic dispersion of the essential cell cycle protein, $p13^{suc1}$, examined in living cells. Proc Natl Acad Sci USA 91: 2176–2180

Hulen D, Baron A, Salisbury J, Clarke M (1991) Production and specificity of monoclonal antibodies against calmodulin from *Dictyostelium discoideum*. Cell Motil Cytoskeleton 18: 113–122

Hush JM, Wadsworth P, Callaham DA, Hepler PK (1994) Quantification of microtubule dynamics in living plant cells using fluorescence redistribution after photobleaching. J Cell Sci 107: 775–784

James P, Vorherr T, Carafoli E (1995) Calmodulin-binding domains: just two faced or multi-faceted? Trends Biochem Sci 20: 38–42

Keith C, DiPaola M, Maxfield FR, Shelanski ML (1983) Microinjection of Ca^{++}-calmodulin causes a localized depolymerization of microtubules. J Cell Biol 97: 1918–1924

Lancelle SA, Callaham DA, Hepler PK (1986) A method for rapid freeze fixation of plant cells. Protoplasma 131: 153–165

Larsen PM, Wolniak SM (1993) Asynchronous entry into anaphase induced by okadaic acid: spindle microtubule organization and microtubule/kinetochore attachments. Protoplasma 177: 53–65

Lee YC, Wolff J (1982) Two opposing effects of calmodulin on microtubule assembly depend on the presence of microtubule-associated proteins. J Biol Chem 257: 6306–6310

Lowry OH, Rosebrough NJ, Farr AL, Randall RJ (1951) Protein measurement with the folin phenol reagent. J Biol Chem 193: 265–275

Matthies HJG, Miller RJ, Palfrey HC (1993) Calmodulin binding to and cAMP-dependent phosphorylation of kinesin light chains modulate kinesin ATPase activity. J Biol Chem 268: 11176–11187

Means AR (1994) Calcium, calmodulin and cell cycle regulation. FEBS Lett 347: 1–4

Melan MA, Sluder G (1992) Redistribution and differential extraction of soluble proteins in permeabilized cultured cells: implications for immunofluorescence microscopy. J Cell Sci 101: 731–743

Miller DD, Lancelle SA, Hepler PK (1996) Actin microfilaments do not form a dense meshwork in *Lilium longiflorum* pollen tube cells. Protoplasma 195: 123–132

Mitsuyama F, Kanno T (1993) Localization of Ca^{2+}-calmodulin to the kinetochore of C6 glioma cells: an investigation of the antitumour effects of calmodulin antagonists in the treatment of brain tumours. Neurol Res 15: 131–135

Muto S, Miyachi S (1984) Production of antibody against spinach calmodulin and its application to radioimmunoassay for plant calmodulin. Z Pflanzenphysiol 114: 421–431

Poovaiah BW, Reddy ASN (1993) Calcium and signal transduction in plants. Crit Rev Plant Sci 12: 185–211

Reddy ASN, Safadi F, Narasimhulu SB, Golovkin M, Hu X (1996) A novel plant calmodulin-binding protein with a kinesin heavy chain motor domain. J Biol Chem 271: 7052–7060

Rhoads AR, Friedberg F (1997) Sequence motifs for calmodulin recognition. FASEB J 11: 331–340

Roberts DM, Harmon AC (1992) Calcium-modulated proteins: targets of intracellular calcium signals in higher plants. Annu Rev Plant Physiol Plant Mol Biol 43: 375–414

Schacterle GR, Pollack RL (1973) A simplified method for the quantitative assay of small amounts of protein in biologic material. Anal Biochem 51: 654–655

Staehelin LA, Hepler PK (1996) Cytokinesis in higher plants. Cell 84: 821–824

Stemple DL, Sweet SC, Welsh MJ, McIntosh JR (1988) Dynamics of a fluorescent calmodulin analog in the mammalian mitotic spindle at metaphase. Cell Motil Cytoskeleton 9: 231–242

Sweet SC, Rogers CM, Welsh MJ (1989) Calmodulin is associated with microtubules forming in PtK_1 cells upon release from nocodazole treatment. Cell Motil Cytoskeleton 12: 113–122

Török K, Whitaker M (1994) Taking a long, hard look at calmodulin's warm embrace. BioEssays 16: 221–224

Valster AH, Hepler PK (1997) Caffeine inhibition of cytokinesis: effect on the phragmoplast cytoskeleton in living *Tradescantia* stamen hair cells. Protoplasma 196: 155–166

Vantard M, Lambert AM, De Mey J, Picquot P, Eldik LJ (1985) Characterization and immunocytochemical distribution of calmodulin in higher plant endosperm cells: localization in the mitotic apparatus. J Cell Biol 101: 488–499

Vos JW, Valster AH, Hepler PK (1998) Methods for studying cell division in higher plants. In: Rieder CL (ed) Structure, composition and function of the mitotic and meiotic spindle. American Society of Cell Biology/Academic Press, London, in press (Methods in cell biology)

Welsh MJ, Sweet SC (1989) Calmodulin regulation of spindle function. In: Hyams JS, Brinkley BR (eds) Mitosis: molecules and mechanisms. Academic Press, London, pp 203–240

– Dedman JR, Brinkley BR, Means AR (1978) Calcium dependent regulator protein: localization in the mitotic apparatus of eukaryotic cells. Proc Natl Acad Sci USA 75: 1867–1871

Wick SM (1990) Localization of calcium-binding proteins in dividing plant cells. In: Leonard RT, Hepler PK (eds) Calcium in plant growth and development. American Society of Plant Physiologists, Rockville, MD, pp 137–143 (The American Society of Plant Physiologists symposium series, vol 4)

– Duniec J (1986) Effects of various fixatives on the reactivity of plant cell tubulin and calmodulin in immunofluorescence microscopy. Protoplasma 133: 1–18

– Muto S, Duniec J (1985) Double immunofluorescence labeling

of calmodulin and tubulin in dividing plant cells. Protoplasma 126: 198–206

Zavortink M, Welsh MJ, McIntosh JR (1983) The distribution of calmodulin in living mitotic cells. Exp Cell Res 149: 375–385

Zhang DH, Wadsworth P, Hepler PK (1990) Microtubule dynamics in living dividing plant cells: confocal imaging of microinjected fluorescent brain tubulin. Proc Natl Acad Sci USA 87: 8820–8824

– – – (1992) Modulation of anaphase spindle microtubule structure in stamen hair cells of *Tradescantia* by calcium and related agents. J Cell Sci 102: 79–89

Zot HG, Aden R, Samy S, Puett D (1990) Fluorescent adducts of wheat calmodulin implicate the amino-terminal region in the activation of skeletal muscle myosin light chain kinase. J Biol Chem 265: 14796–14801